Uncertainties on reactivity for UO_2 and MOX systems due to nuclear data

D. Rochman [a], A.J. Koning [a], D.F. da Cruz [a], and H. Sjöstrand [b]

[a] *Nuclear Research and Consultancy Group NRG, Petten, The Netherlands*

[b] *Department of Physics and Astronomy, Uppsala University, Uppsala, Sweden*

Abstract

This paper presents a global study on the impact of nuclear data for reactivity parameters for different systems and fuels as a function of burn-up. The considered models range from assemblies to full core, for 15 different reactor types, including Generations II, III and IV, with UO_2 or MOX fuel, simulated with the Monte Carlo transport code SERPENT. The impact of ^{235,238}U, ^{239}Pu, fission products, fission yields, other actinides and thermal scattering data is separately considered with the "fast Total Monte Carlo" uncertainty propagation method. The total uncertainties on the reactivity swing are then calculated up to 55 GWd/tHM together with the contributions of each important nuclear data.

1 Introduction

Nowadays, the neutronics experience with UO_2 fuel and thermal reactors such as Pressurized Water Reactors(PWR) is extremely extensive. In MOX cores, the large amount of high-content Plutonium modifies the neutronic system behavior, compared to conventional UO_2 loading [1, 2]. The validations of many system simulations were renewed and consequent efforts have lead to many studies around the world (see for instance Refs. [3–5]). Regarding the uncertainties on such calculations due to input parameters such as nuclear data, all studies are based on sensitivity methods and therefore rely on the availability of covariance files, with an emphasis on the main three actinides (^{235,238}U and ^{239}Pu: see for instance Refs. [6, 7]).

As a complement to previous studies, this paper presents the uncertainties on k_{eff} as a function of burn-up for 15 different nuclear systems, due to an exhaustive list of nuclear data. The same nuclear data and method are used for the considered realistic systems (6 thermal with UO_2 fuel, 5 thermal with MOX fuel and 4 fast systems). The method of uncertainty propagation is based on Monte Carlo principles with the "fast Total Monte Carlo" method

13 January 2014

and does not rely on the availability of covariance files.
The considered simulated systems are first presented, followed by a description of the uncertainty propagation method. The uncertainties on the reactivity swing (total and partial) will follow.

2 Assembly models with SERPENT

A few simple assemblies are considered in this work, based on descriptions available for the transport and burn-up Monte Carlo code SERPENT [8]. The considered cases are well representative of the existing nuclear systems, with some comparisons for future possible concepts. Table 1 presents the different types of assemblies and cores with their fuel contents for which calculations are performed. For the complete description of the assembly characteristics, see the mentioned references.

Additionally, different types of fuel composition can be used for a given system, such as a PWR, *i.e.* UO_2 or MOX fuel. In the case of MOX fuel, Table 2 presents the average isotope concentrations used in the models, obtained from references mentioned in Table 1. Depending on the complexity of the models, these concentrations can be unique, or can differ depending on different zones or assemblies (as in the case of the PWR MOX with 4 types of assemblies).

2.1 Monte Carlo code SERPENT

The three-dimensional continuous-energy Monte Carlo reactor physics burn-up calculation code SERPENT is used for this study [8]. It includes state-of-the-art neutronics software and a point depletion (or burn-up) module, and it keeps track of the nuclide mixture for each of the user-defined depletion zones. Different burn-up zones are used in the models, and in the case of assemblies, periodic boundary conditions are used in all three directions, for setting up an infinite lattice of fuel elements. During the burn-up calculations the predictor-corrector method is used, and source normalization is performed assuming a given power density. The radioactive decay and fission yield data used are read from data libraries in ENDF format. For each model, the burn-up is calculated up to 55 GWd/tHM, followed by different cooling times. Together with the reactivity coefficients as a function of burn-up, the simulations also provide the evolution of number densities during and after burn-up. These calculated data can also be used to provide uncertainties, but are not presented in this paper.
In the following, short descriptions for the considered models are presented. We recommend the mentioned references for detailed descriptions.

Table 1
Type of assemblies and cores with different fuel compositions considered in this work. The mentioned references provide the SERPENT input descriptions for each system.

System types		configuration	average fuel content		Ref.
			^{235}U	Pu	
1	PWR MOX-r	assemblies	0.2 %	4.3 %	[9]
2	PWR MOX-w	assemblies	0.2 %	4.3 %	[10]
3	PWR UO_2 + Gd	assembly	4.0 %	-	[11]
4	PWR UO_2	assembly	4.8 %	-	[12]
5	BWR UO_2 + Gd	assembly	4.0 %	-	[13]
6	BWR MOX + Gd	assembly	0.4 %	3.9 %	[13]
7	VVER UO_2	assembly	3.6 %	-	[14]
8	VVER MOX	assembly	0.2 %	4.1 %	[15]
9	EPR MOX	assemblies	0.2 %	4.3 %	[16]
10	CANDU	assembly	0.7 %	-	[17]
11	AGR	assembly	2.2 %	-	[18]
12	ELECTRA LFR Pu	full core	-	91 %	[19]
13	SFR	assembly	0.01	20 %	[20]
14	ADS	full core	-	43 %	[20]
15	GCFR	full core	0.6	14/17 % (inner/outer core)	[21]

2.2 PWR UO_2, with and without Gd

The model without gadolinium (Gd) is fully described in Refs. [11, 12]. The PWR fuel element used in this work is based on a Westinghouse 3-loop PWR design. The fuel element consists of an array of 17x17 of these rods with a pitch of 1.26 cm. This typical PWR fuel element is 4 m in length and 21.5 cm in width, and contains some 400-500 kg of enriched uranium. The enrichment is 4.8 % in ^{235}U. The uranium oxide ceramic pellets are inserted into the Zircaloy (cladding material) with diameter of 0.95 cm and thickness of 0.65 mm. The pellet diameter is 0.82 cm.
The temperature of the fuel is assumed to be 930 Kelvin, and that of the cladding and moderator/coolant 586 Kelvin. The boric acid concentration in the coolant is taken to be constant during the entire depletion period and equal to 500 ppm. A total of 39 burn-up zones are used in our model, one for

Table 2
Average MOX fuel compositions in percent with different isotopes for the considered systems. The percentage is in mass of heavy metals.

System types	^{235}U	^{238}U	^{238}Pu	^{239}Pu	^{240}Pu	^{241}Pu	^{242}Pu	Other
PWR MOX-r	0.22	95.38	0.04	2.93	0.91	0.33	0.12	<0.1
PWR MOX-w	0.22	95.37		4.13	0.26	0.02	0.004	
BWR MOX+Gd	0.39	93.07	0.14	3.05	1.95	0.87	0.53	
VVERMOX	0.20	95.68	0.03	2.75	0.86	0.31	0.12	< 0.1
EPR MOX	0.22	95.48	0.18	2.16	1.01	0.53	0.42	< 0.1
ELECTRA	-	-	3.47	51.75	23.83	11.76	7.98	1.21
SFR	0.01	80.50	0.07	10.44	4.79	2.60	1.59	
GCFR	0.60	85.19	0.38	7.96	3.67	1.05	1.04	<0.1
ADS			1.61	20.06	14.80	1.67	5.18	56.68

each fuel rod and assuming a 45-degree symmetry. Each fuel zone is considered as a single burn-up zone, therefore not subdivided in annular sub-zones. A periodic boundary condition is used in all three directions, for setting up an infinite lattice of fuel elements (see Fig. 1). During the burn-up calculations the predictor-corrector method is used, and source normalization is performed assuming a power density of 39.0 W/g.
The information used for the assembly model with Gd are given in Ref. [11] related to the Japanese Post Irradiation Experiment from the TAKAHAMA-3, a 17x17 PWR assembly. This assembly is loaded with 248 UO_2 fuel pins, 4.1 %wt ^{235}U enriched, 16 UO_2-Gd_2O_3 pins (2.6 % wt ^{235}U and 6 % wt Gd) and 25 water holes. The fuel pin pitch is 1.26 cm, the fuel clad radius 0.47 cm, the fuel pellet radius 0.40 cm and the cladding thickness is 0.072 cm. The fuel temperature is 900 K, 600 K for the cladding temperature and 576 K for the moderator temperature. There are 25 guide tubes modeled as water-filled zircalloy tubes with an outer radius of 0.61 cm and an inner radius of 0.57 cm.

2.3 PWR and EPR MOX

The models of PWR MOX-r (for reactor-grade Pu) and MOX-w (weapon-grade Pu) as described in Ref. [8] are used in the following, with the design derived from Ref. [9] ([10] for the MOX-w content). Four types of assemblies with different concentrations of Pu are used: (1) UO_2 fuel, initially enriched at 3.2 % and originally burned at 25 MWd/kgU (including heavy actinides and fission products, (2) MOX fuel with a low Pu enrichment of 2.9 %, (3) MOX

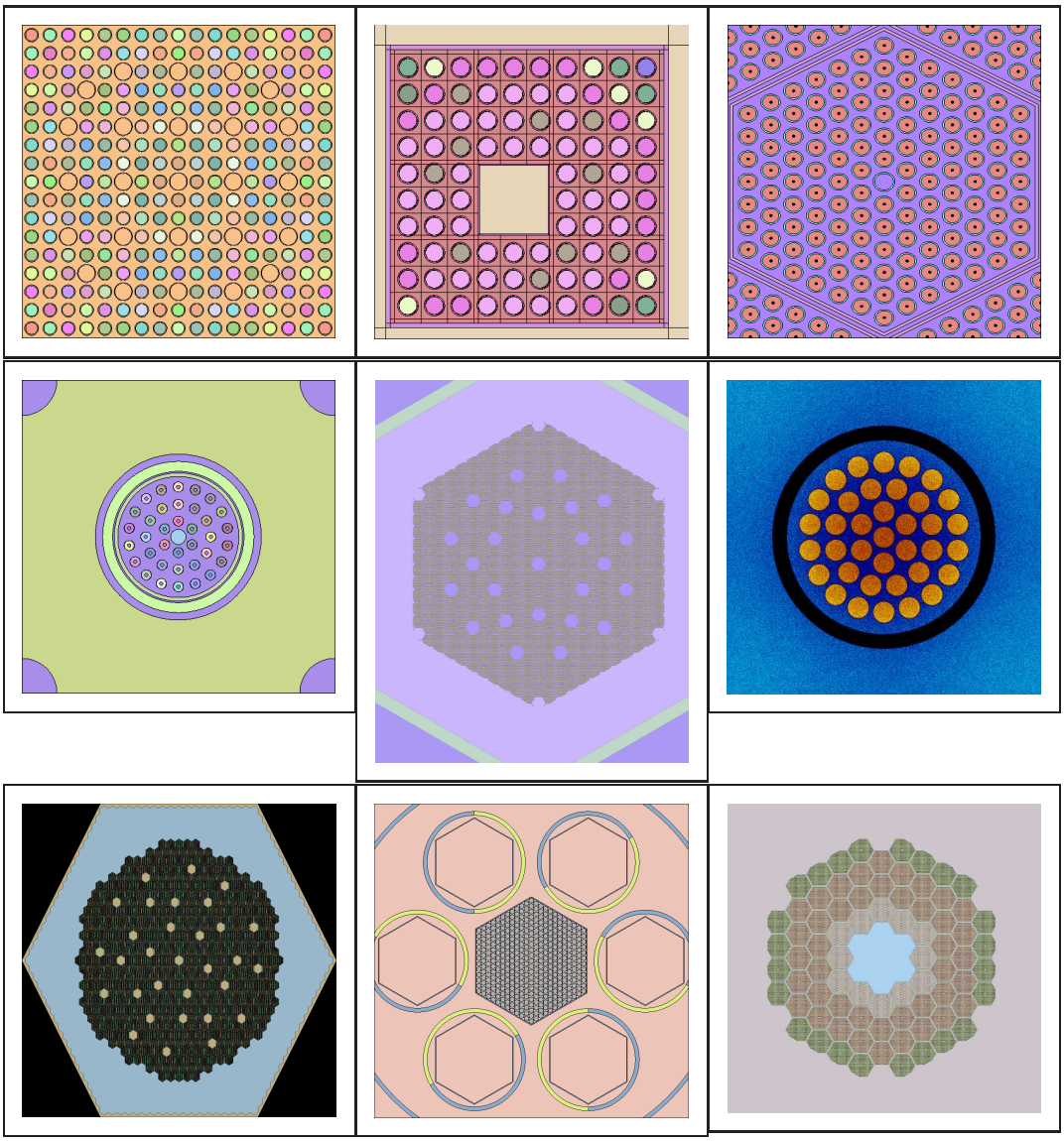

Fig. 1. From the top left to bottom right: (1) PWR assembly with UO_2 fuel, (2) BWR assembly with UO_2 fuel, (3) VVER assembly with UO_2 fuel, (4) AGR assembly, (5) SFR assembly, (6) CANDU assembly, (7) cross section of the GCFR core, (8) cross section of the ELECTRA core, and (9) cross section of the ADS core.

fuel with a medium Pu enrichment of 4.4 % and (4) MOX fuel with a high Pu enrichment of 5.6 %. The model of the EPR MOX assembly is based on available pre-design data from Ref. [16], using dimensions similar to the PWR MOX-r. The same four types of assemblies were used with different concentrations of Pu (2.9 %, 4.4 % and 5.6 %). The plutonium vector is presented in Table 2, obtained from Ref. [16]. Note that it is significantly different from to the one for PWR MOX-r. Although these data might not be the ones used during the final design of a "real" EPR core, it corresponds to the available information at the present time.

2.4 BWR UO_2 and MOX

The description of the asymmetric BWR assembly with UO_2 and Gd fuel is presented in Refs. [13, 22]. The geometry which is representative of modern 10x10 BWR fuel consists of four ATRIUM-10 (10-9Q) assemblies centered around a cruciform control blade position in a 2x2 control cell, which constitutes the basic repeating unit of the core. The fissile content is set at a level such that the assembly is capable of reaching equilibrium discharge burn-ups of up to 50 MWd/kgHM. The 10x10 assembly contains 7 different rod types with different ^{235}U enrichment levels (from 2.2 to 4.8 %) and one rod type with Gd_2O_3 (4.3 % ^{235}U and 3.0 % Gd_2O_3). The average lattice enrichment is 4 % (see Fig. 1 right).
Similar to the BWR UO_2 assembly, the MOX assembly follows the descriptions given in Ref. [13]. The MOX fuel rods have a density of 9.921 g/cm^3 with the isotopic vector as presented in Table 2.

2.5 VVER UO_2 and MOX

The full specifications of geometry and material compositions are found in Ref. [14] and the details are not repeated here. An average fuel enrichment of 3.6 % in weight is used for the full assembly. The dimensions of the assemblies are similar to real VVER-440 fuel, with the active height reduced to 125 cm (see Fig. 1). The concentration of boron is kept constant during the full burn-up calculation, and equal to 650 ppm.
The MOX assembly characteristics in this work are defined in Refs. [15, 23]. The standard MOX assembly used includes three zones with different Pu contents. The listed initial MOX composition is a representative of the realistic UOX fuel irradiated in a mixed MOX-UOX LWR core. This MOX fuel consists of a typical plutonium vector for material derived from reprocessing of thermal reactor UOX fuel. The plutonium isotopic composition, corresponding to the three Pu content zones is as follows: ^{238}Pu 0.8 %, ^{239}Pu 66.7 %, ^{240}Pu 20.6 %, ^{241}Pu 7.5 %, ^{242}Pu 2.9 %. Three different Pu contents are used in the MOX fuels: high (5.5 %), medium (4.3 %) and low (2.8 %). The uranium isotopic composition corresponds to depleted uranium.

2.6 AGR assembly

The AGR model is based on data for the 2x660 MWe Torness power plant [18], a second generation of AGRs. When data were not available for this plant in open literature, corresponding data from other AGR plants were used. A square super-cell model with 46x46 cm^2 area has been implemented (see

Fig. 1), which comprised of a single fuel assembly within a graphite fuel channel, and surrounded by four core channels placed in interstitial positions (the four corners of the square). These interstitial channels are supposed to be filled with the CO_2 coolant. The fuel assembly is consisted of 36 fuel pins surrounded by two concentric graphite sleeves. The fuel pins are filled with pellets of UO_2 fuel with 2.2 % enrichment and external diameter 14.5 mm. The cylindrical pellets contain a central hole. Stainless steel has been used as cladding material. An average fuel rating of 13.65 MW/tHM has been considered for the depletion calculations. Each of the 36 fuel pins are depleted individually, and the cell model has reflective boundaries on all its sides.

2.7 CANDU UO_2

Detailed descriptions of the model can be found in Refs. [8, 17]. The SERPENT model as presented in these references is used, without modifications. In this design, the channel is composed of a stainless steel liner followed by an insulator of zirconia and of a pressure tube made of a zirconium alloy. The fuel is made of natural uranium (0.7 % ^{235}U). The central pin is filled with light water. Light water is used as coolant and heavy water as moderator. The lattice pitch is set to 18.2 cm (see Fig. 1 right).

2.8 Generation-IV systems

Future systems (Generation-IV reactors) are considered in this study as their preliminary designs often include a high amount of plutonium isotopes and minor actinides, which can have a large impact on k_{eff} and its uncertainties.

- SFR assembly
  The geometry of fuel pin, sub-assembly and other core inner structures was adopted from the reference BN600 design fully loaded with UOX [20]. In order to maintain the multiplication factor above unity during burn-up, 20 at.% Pu was introduced into the MOX fuel for present core design. This core consists of 369 driver sub-assemblies. Each fuel sub-assembly is loaded with 127 fuel pins and one stainless steel rod in center (see Fig. 1).
  Pin pitch and sub-assembly pitch is equal to 8 mm and 99 mm respectively (see Ref. [20, 24]). The isotopic composition of Pu and Am were obtained from spent fuel discharged from LWR with 50 MWd/kgHM burn-up after 5 years of cooling. The cladding material adopted for BN600 is the steel cladding ChS-68.
- ADS core
  The description of the core model can be found in Refs. [20,25]. The geometry of fuel pins and sub-assemblies loaded into the suggested ADS design was

derived from the reference EFIT-400 design loaded with ceramic-ceramic fuel (except some modifications aiming at a higher neutron source efficiency (see Fig. 1). The atomic fraction of Pu in heavy mass isotopes was fixed to 43.5%. The minor actinide inventory consists of Np (4.0 at.%), Am (91.8 at.%) and Cm (4.2 at.%).

- ELECTRA core
  ELECTRA stands for "European Lead Cooled Training reactor" and is a 0.5 MW lead cooled training reactor [19]. The fuel consists of uranium-free nitride fuel (plutonium-zirconium-nitride (Pu,Zr)N) in a sealed fuel cycle. The fuel pellet diameter is 11.5 mm.The Pu vector comes from spent PWR UOX fuel with a burn-up of 43 GWd/ton, allowed to cool for four years before reprocessing, and two years before loading into the here investigated core: 3.5 % of ^{238}Pu, 51.9 % ^{239}Pu, 23.8 % ^{240}Pu, 11.7 % ^{241}Pu, 7.9 % ^{242}Pu and 1.2 % ^{241}Am. The control assemblies were assumed to consist of B_4C pins enriched to 90 % in ^{10}B. The active core dimensions are 30 x 30 cm, with shutdown and reactivity compensation using 6 rotating "drums" with 180 degree B_4C sectors (see Fig. 1).
- GCFR core
  The design characteristics of a pin fueled core with silicon-carbide ceramic cladding for the 2400 MWth Gas-cooled Fast Reactor was obtained from the GoFastR (Gas-cooled Fast Reactor) project [21] (see Fig. 1). The SERPENT input description can be found in Ref. [21].

3 Uncertainty propagation with the fast TMC method

In the following, we will describe the method applied for uncertainty propagation and the type of nuclear data.

3.1 The fast TMC method

The full description of the original TMC method can be found in Ref. [26], with an important upgrade in Ref. [27], leading to the fast TMC method. Only the main outlines will be repeated here. In the case of Monte Carlo transport simulations, the fast TMC method takes advantages of associating the randomization of nuclear data inputs together with the random source neutrons. It simply consists of repeating identical calculations with each time different random nuclear data files and random seeds for random number generator of the Monte Carlo transport code. Additionally, the neutron history for each random calculation is relatively small: if m neutron histories are desirable to obtain a sufficiently small statistical uncertainty for a given calculation (for instance 50 pcm for k_{eff}), then each random set is using m/n neutron histories,

n being the number of random files. In Ref. [27], it is advised to take $n = 300$. m/n should not be too small, and n can be decreased to obtain an acceptable m/n value. The obtained spread in a calculated quantity will then reflect the spread of input parameters such as nuclear data.
It is emphasized that while the original TMC method can be applied to both Monte Carlo and deterministic reactor codes, fast TMC can only be applied to Monte Carlo codes. This method can be applied to quantities during burn-up calculations: k_{eff}, nuclide inventory, reaction rates, grouped cross sections, *etc.* As fast TMC will be applied with the Monte Carlo transport and depletion code SERPENT, the observed spread (for instance in k_{eff}) can be related to nuclear data with the following equation:

$$\sigma^2_{\text{observed}} = \sigma^2_{\text{nuclear data}} + \overline{\sigma}^2_{\text{statistics}} \tag{1}$$

In the following, σ is the standard deviation of a distribution and will be used for the definition of uncertainty. σ_{observed} is the observed standard deviation from the n realizations of the same SERPENT calculation, each time with different nuclear data. $\sigma_{\text{nuclear data}}$ is the uncertainty on the calculated quantity due to the variations of nuclear data. $\overline{\sigma}_{\text{statistics}}$ is the statistical uncertainty from the m/n neutron history.
If σ_{observed} is simply "*observed*", $\overline{\sigma}_{\text{statistics}}$ needs to be calculated. In the case of quantities provided by SERPENT with their own statistical uncertainty like k_{eff}, $\overline{\sigma}_{\text{statistics}}$ can be obtained with the following equation:

$$\overline{\sigma}_{\text{statistics}} = \frac{1}{n}\sqrt{\sum_{i=1}^{n} \sigma^2_{\text{statistics,i}}} \tag{2}$$

$\sigma_{\text{statistics,i}}$ is the statistical uncertainty provided by SERPENT for the run i, with i from run 1 to n. Eq. (2) is valid if the seed of the random number generator of the Monte Carlo transport part of the code is changed for each run. In the case of the original TMC description, the seed is set to a unique value for all the n runs, making the use of Eq. (2) not the best estimator of $\sigma_{\text{statistics}}$.
In the case of quantities not provided with their own statistical uncertainties, such as number densities for the isotope inventory, one needs to independently evaluate $\sigma_{\text{statistics,i}}$. In this case, n calculations are also realized, but only changing the seed. Thus, the spread in the observed quantity is only due to the statistics.
Finally, in the case of possible bias in $\sigma_{\text{statistics,i}}$ (as explained in Ref. [27]), the independently evaluation of $\sigma_{\text{statistics,i}}$ is recommended.

In practice, the following is performed:

(1) perform a first SERPENT calculation for a given geometry and all nuclear data set to ENDF/B-VII.1, with $m = 2000 \times 500$ (2000 neutron histories for 500 cycles) to obtain reference values. This run is not mandatory, but

can be used to verify that the fast TMC method leads to correct central values,

(2) apply the fast TMC method: repeat the same calculation n times (n from 100 to 300, depending on the convergence rate of the uncertainties), with each time different random seeds and nuclear data (see next section for the type of nuclear data). Each calculation is performed with m/n neutron histories,

(3) extract k_{eff} distributions and use Eqs. (1) and (2) to extract $\sigma_{\text{nuclear data}}$.

Burn-up calculations are performed up to 55 GWd/tHM, followed by cooling time. In each burn-up step, the random nuclear data are used, thus propagating the effect of nuclear data through depletion steps.

3.2 Type of nuclear data

One of the advantages of the fast TMC method is to allow for the variations of any type of nuclear data, without the need of covariance data, in the form of an ENDF file (with its inherent restrictions). In this work, both nuclear data for transport and depletion will be randomly changed. They are produced with the TALYS system [28], designed for the production of nuclear data files. The following data are considered:

- cross sections, neutron emission, neutron and gamma spectra and angular distributions for the main actinides ^{235,238}U and ^{239}Pu. It corresponds to the entire ENDF-6 file,
- thermal scattering data for H in H_2O, D in D_2O and C in graphite
- cross sections, neutron emission, neutron and gamma spectra and angular distributions for fission products (89 fission products are varied all together: $^{72-74}$Ge, ^{75}As, ^{76}Ge, ^{77,78}Se, ^{79}Br, ^{80}Se, ^{81}Br, ^{82}Se, ^{83,84}Kr, ^{85}Rb, ^{86}Kr, ^{87}Rb, ^{88}Sr, ^{89}Y, $^{90-92}$Zr, ^{93}Nb, ^{94}Zr, ^{95}Mo, ^{96}Zr, ^{97,98}Mo, ^{99}Tc, ^{100}Mo, ^{101,102}Ru, ^{103}Rh, ^{104}Ru, $^{105-108}$Pd, ^{109}Ag, ^{110}Pd, $^{111-114}$Cd, ^{115}In, ^{116}Cd, $^{117-120}$Sn, ^{121}Sb, ^{122}Sn, ^{123}Sb, ^{125,126}Te, ^{127}I, ^{128}Te, ^{129}I, ^{130}Te, ^{131,132}Xe, ^{133}Cs, ^{134,135}Xe, ^{135}Cs, ^{135}Ba, ^{136}Xe, ^{137,138}Ba, ^{138,139}La, ^{140}Ce, ^{141}Pr, ^{142}Ce, $^{143-146}$Nd, ^{147}Sm, ^{148,150}Nd, ^{151}Eu, ^{152}Sm, ^{153}Eu, ^{154}Sm, $^{155-158,160}$Gd),
- cross sections, neutron emissions, neutron and gamma spectra and angular distributions for other actinides (15 actinides are varied all together: ^{234,236,237}U, ^{237}Np, ^{238,240,241,242}Pu, ^{241,242g,243}Am, ^{242,243,244,245}Cm),
- fission yields for important actinides: ^{234,235,236,238}U, ^{239,240,241}Pu, ^{237}Np, ^{241,243}Am and ^{243,244}Cm at different incident neutron energies.

Nuclear data are either varied together or independently, depending on their importance. For instance, all fission products are randomly changed at once, whereas the thermal scattering data and main actinides nuclear data are sep-

arately changed.
In SERPENT, the nuclear data for transport and depletion calculations are both read from the same source, being the ACE files, obtained after processing of the ENDF-6 files with the NJOY code. The same processing is applied for each type of nuclear data. The random nuclear data files used in the following were already tested for ^{235,238}U, ^{239}Pu, thermal scattering data for H in H_2O, fission products and fission yields. Results can be found in Refs. [12, 29–35]. The random thermal scattering data for D in D_2O and C in graphite are used for the first time in this study. The procedure to produce these random files is similar to the one for H in H_2O (see Ref. [32]). The same model parameters are varied, with half the uncertainties for all of them to obtain similar effects compared to H in H_2O variations. The impact of the parameter uncertainties was tested on criticality benchmarks: *e.g.* the spread of C in graphite for the leu-comp-therm-060 benchmark [36] (a RBMK system) was about 700 pcm and the one of D in D_2O for leu-met-therm-001 400 pcm. These random thermal scattering data are available online [37].

4 Results

4.1 k_{eff} total uncertainties

The total uncertainties on k_{eff} due the varied nuclear data are presented in Fig. 2. The results for current reactors and Generation-III are separately presented depending on the fuel type. The following general remarks can be done based on these results:

(1) all thermal systems have k_{eff} uncertainties in the range of 0.55 to 0.95 %,
(2) the uncertainties for thermal systems with UO_2 fuel tend to increase as a function of burn-up, showing a structure around 5-10 GWd/tHM when Gd is present,
(3) the uncertainties for thermal systems with MOX fuel are constant or decreasing, with a flatter behavior than for the UO_2 cases, and
(4) the uncertainties for fast systems are relatively high and virtually constant (above 1 %).

To better understand these behaviors, the individual effects of each important nuclear data need to be analyzed, as presented in the next section. It is nevertheless worth noticing that thermal systems present lower uncertainties than fast systems, and that the uncertainties for UO_2 and MOX fuels are relatively similar. This observation is confirmed in Ref. [38], where a study on a pincell level between UO_2 and MOX fuels also show comparable results.

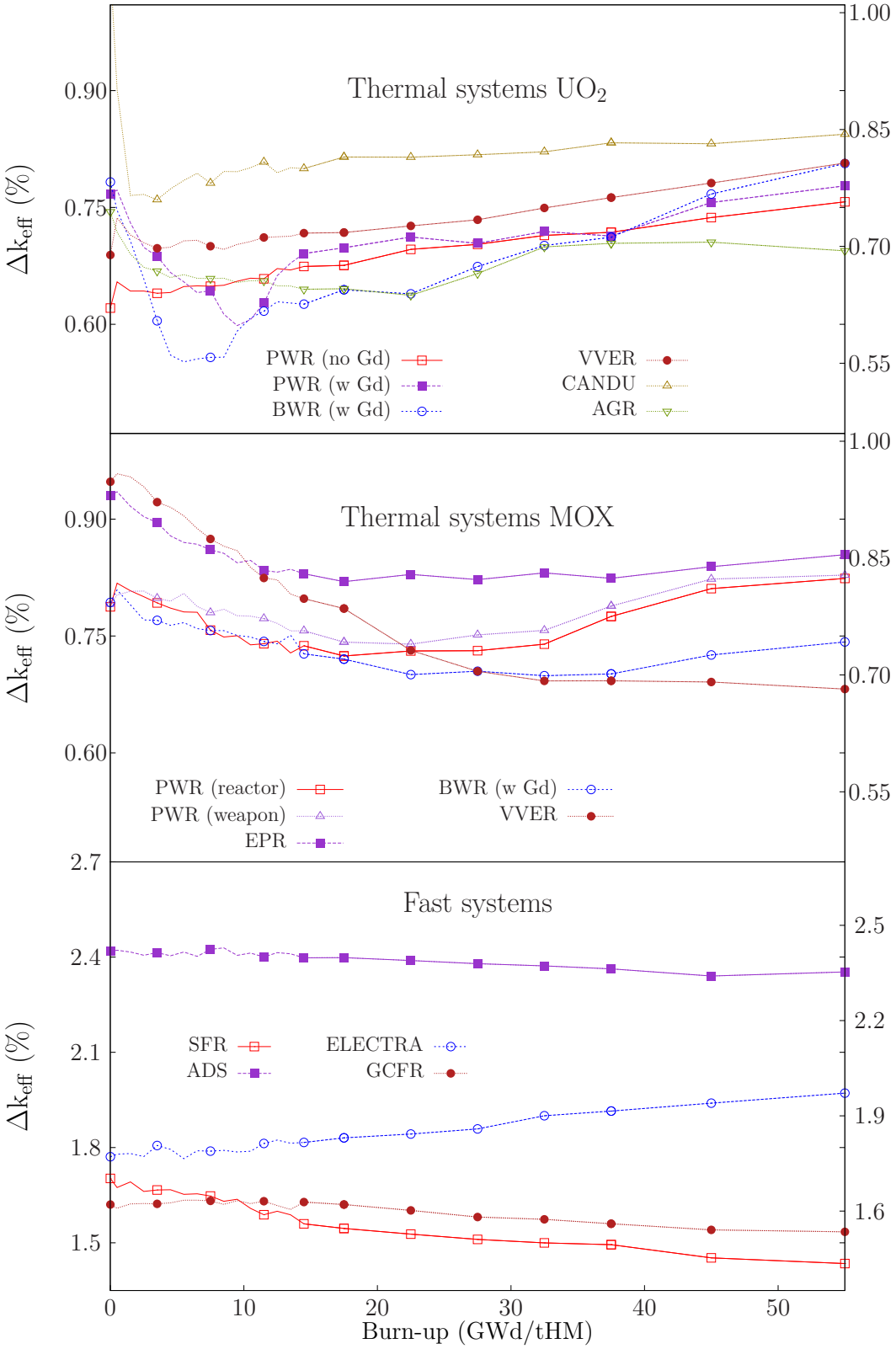

Fig. 2. k_{eff} uncertainties in percent due to ^{235,238}U, ^{239}Pu, thermal scattering data, fission products, other actinides and fission yields.

4.2 k_{eff} partial uncertainties

The fast TMC method allows to disentangle the origins of the uncertainties by either varying nuclear data separately (as performed in this work), or by using correlations between nuclear data and the calculated quantities (as shown in Ref. [39]). Figs. 3 to 5 present the relative contributions to the k_{eff} uncertainties (normalized to 100 %) for the different considered systems. A few common remarks can be mentioned:

(1) the main contributors to the k_{eff} uncertainties during the complete burn-up are ^{235}U, ^{238}U and ^{239}Pu,
(2) the effect of other actinides become more important are high burn-up, but are of minor importance (except when they are present in the initial fuel, as for Generation-IV systems and BWR with MOX fuel),
(3) fission products are of secondary importance, apart when they are present in the initial fuel, as for Gd,
(4) fission yields have a non-negligible impact at the end of cycle,
(5) the cladding effect on k_{eff} is small (less than 100 pcm at all burn-up rate),
(6) and finally the thermal scattering data are an important source of uncertainty, with specific behavior as a function of the burn-up rate.

Other specific remarks can be reported:

- It is interesting to notice the effect of gadolinium in the two considered PWR assemblies (see Figs. 2 and 3, PWR with and without Gd): at low burn-up, the total uncertainties are modified (up to 10-15 GWd/tHM), showing an additional structure when the Gd is present. The presence of Gd isotopes in the fuel is shifting the neutron flux energy towards thermal values (as a burnable neutron absorber), increasing the effect of the thermal scattering data (as seen in Fig. 3). At higher burn-up, the effect of Gd is diminishing together with its concentration.
- The thermal scattering data, which are usually not included in uncertainty analysis, show an important impact with specific behavior depending on the considered system. For fast reactors (SFR, ADS, ELECTRA and GCFR), there is no impact from thermal scattering, but in almost all the other systems (except for BWR UO_2), the effect of the thermal scattering data should not be neglected. In the case of MOX fuel, because of the resonances in the thermal range for ^{239}Pu, ^{240}Pu and ^{241}Pu, changes in thermal scattering data can have a high effect on reaction probabilities [38]. Additional studies should be performed on the impact of thermal scattering data to better quantify their relations with the neutron spectrum.
- For fast systems, the present study is showing a more simple effect of nuclear data on k_{eff}, with a predominant source of uncertainties from ^{239}Pu and other minor actinides. For such fuels (high percentage of plutonium

isotopes), additional efforts are needed at the level of nuclear data evaluations and measurements of basic differential quantities to obtain acceptable uncertainties for system design [40]. The partial uncertainties for the GCFR and ADS systems are not included in the figures, but are very similar to the ones for the SFR and ELECTRA systems, respectively.
It was shown in Ref. [41] that in the case of ELECTRA, a large contribution in the uncertainty of k_{eff} is due to the uncertainty in the coolant (Pb). A similar effect might be found for other fast systems, since the coolant is not water.

- With the use of MOX fuel, the impact of minor actinides is increased compared to UO_2. It is compensated by a lower impact of ^{235}U, leading to similar total k_{eff} uncertainties between UO_2 and MOX fuel.
- In the case of the AGR assembly, the thermal scattering data of relevance are C in graphite. As this system contains graphite as a moderator, the quantity of graphite is relatively large, reflected by the k_{eff} uncertainties due to these scattering data (see Fig. 5), especially at the beginning of cycle.
- As for AGR assembly, the thermal scattering data of relevance for the CANDU assembly are D in D_2O. The behaviors of the uncertainties due to D in D_2O and C in graphite are relatively different than of H in H_2O and more studies should be performed to understand the changes (for instance, with criticality benchmarks).

4.3 Other remarks

The comparison of uncertainties necessitates care and understanding of the methods used to produce them. It is more straightforward to compare cross sections or k_{eff}, since in principle there is only one correct value. But uncertainties (and correlations) are the expression of the methods applied to obtain them. Therefore there are theoretically no erroneous uncertainties, as long as justifications can be provided.
It was recently mentioned that the calculated uncertainties (in the vicinity of 0.8 %) are higher than the global bias between the calculated k_{eff} and the benchmark values for lattice physics codes for PWR and BWR fuels (about 0.2 %) [42]. Additionally, it was noticed that *"Reactor operation data, such as core start-up tests, core surveillance measurements of reaction rates, critical boron measurements in PWR or critical control rod patterns in BWR, indicate much smaller calculational uncertainties"* (than obtained from methods as used in this work) [42]. These remarks, obtained from experiences in the applied calculations compared to integral experimental data, are worth noticing. To better understand these differences, it is useful to mention that the nuclear data included in libraries (as for instance in ENDF/B-VII [43], JENDL-4 [44], or TENDL [45]) are often adjusted to differential (*e.g.* cross

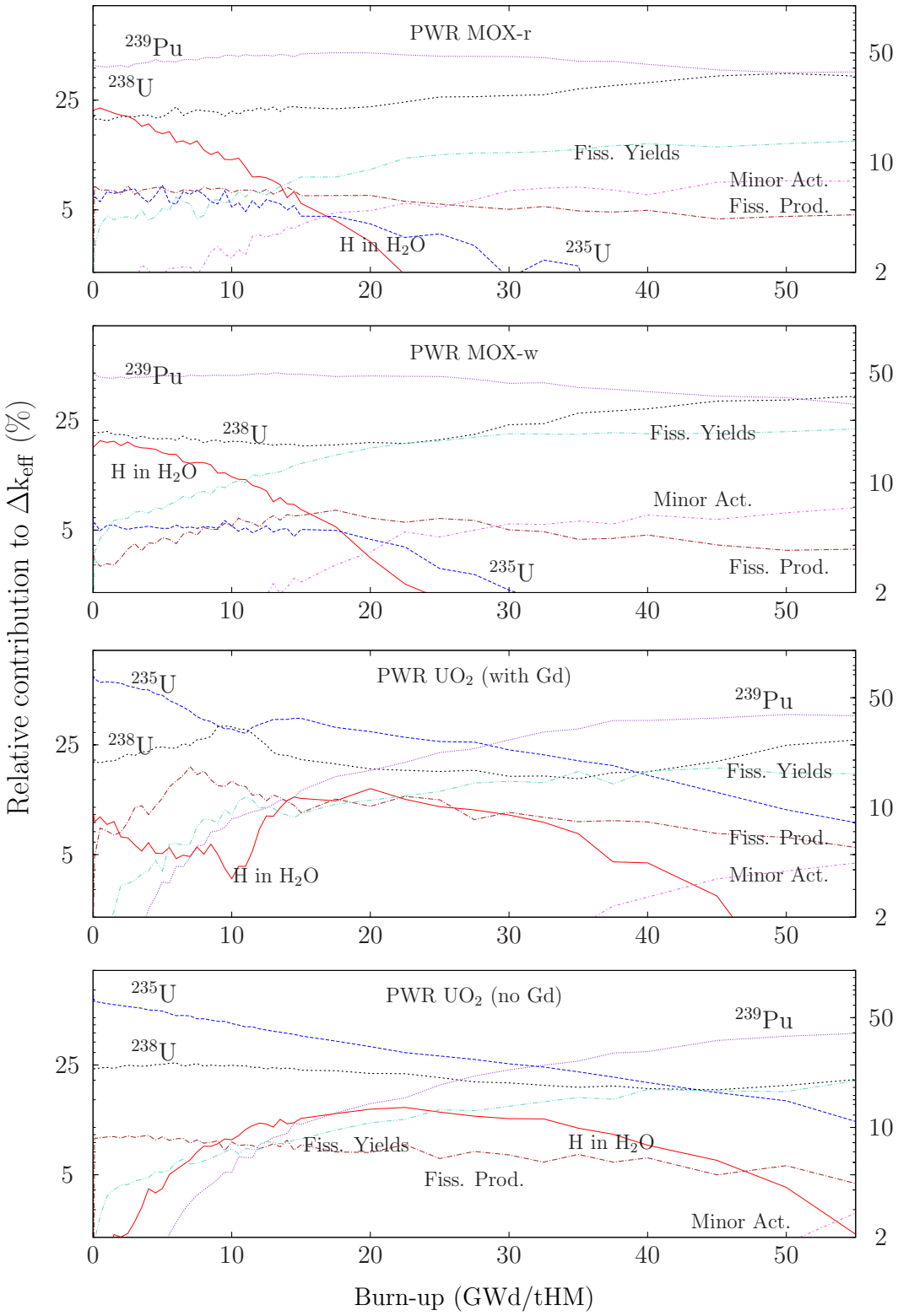

Fig. 3. k_{eff} uncertainties for PWR assemblies, with different types of fuels. Uncertainties are due to ^{235,238}U, ^{239}Pu, H in H_2O thermal scattering data, fission products, other actinides and fission yields.

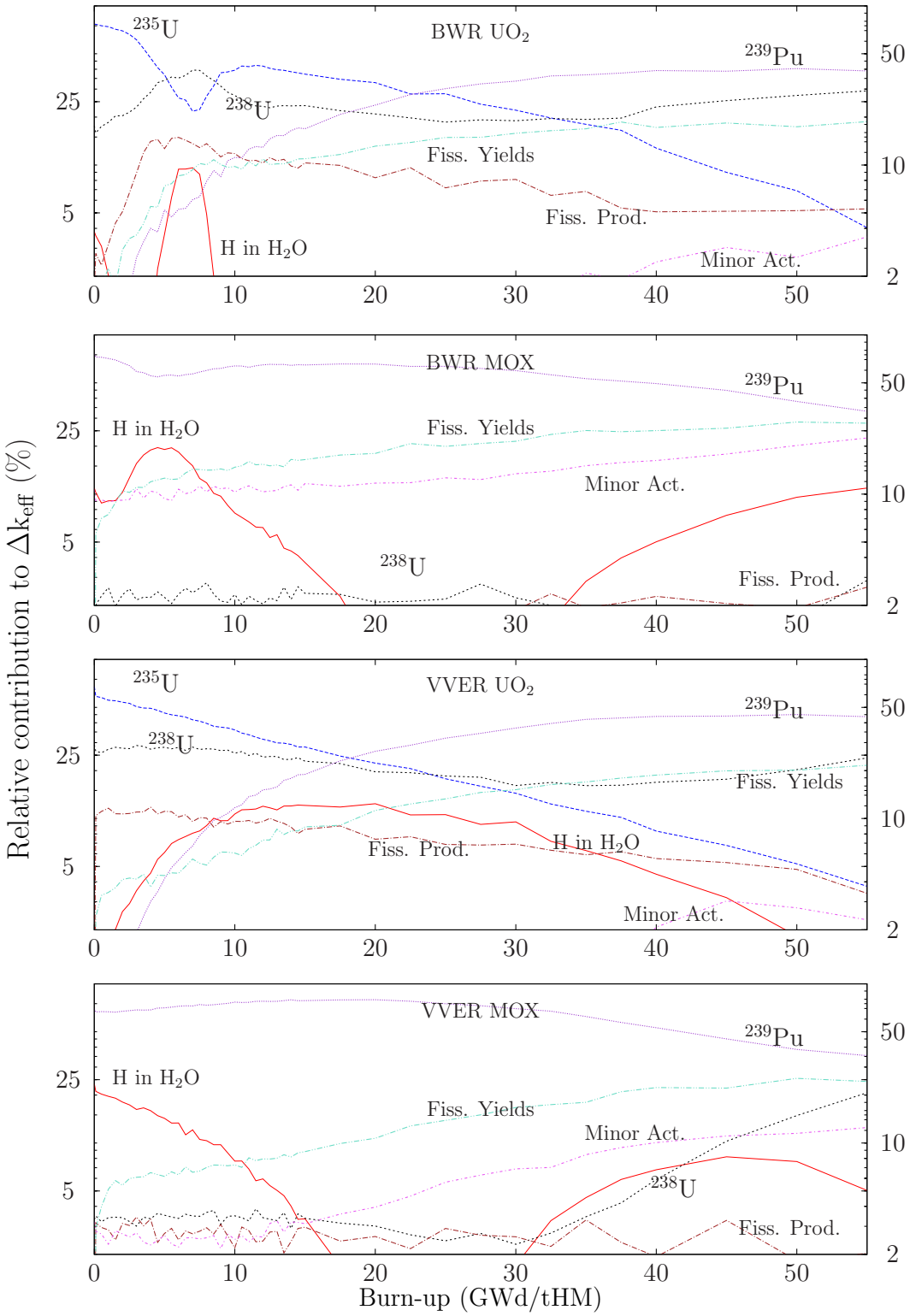

Fig. 4. k_{eff} uncertainties for BWR and VVER assemblies, with UO_2 and MOX fuels. Uncertainties are due to $^{235,238}U$, ^{239}Pu, H in H_2O thermal scattering data, fission products, other actinides and fission yields.

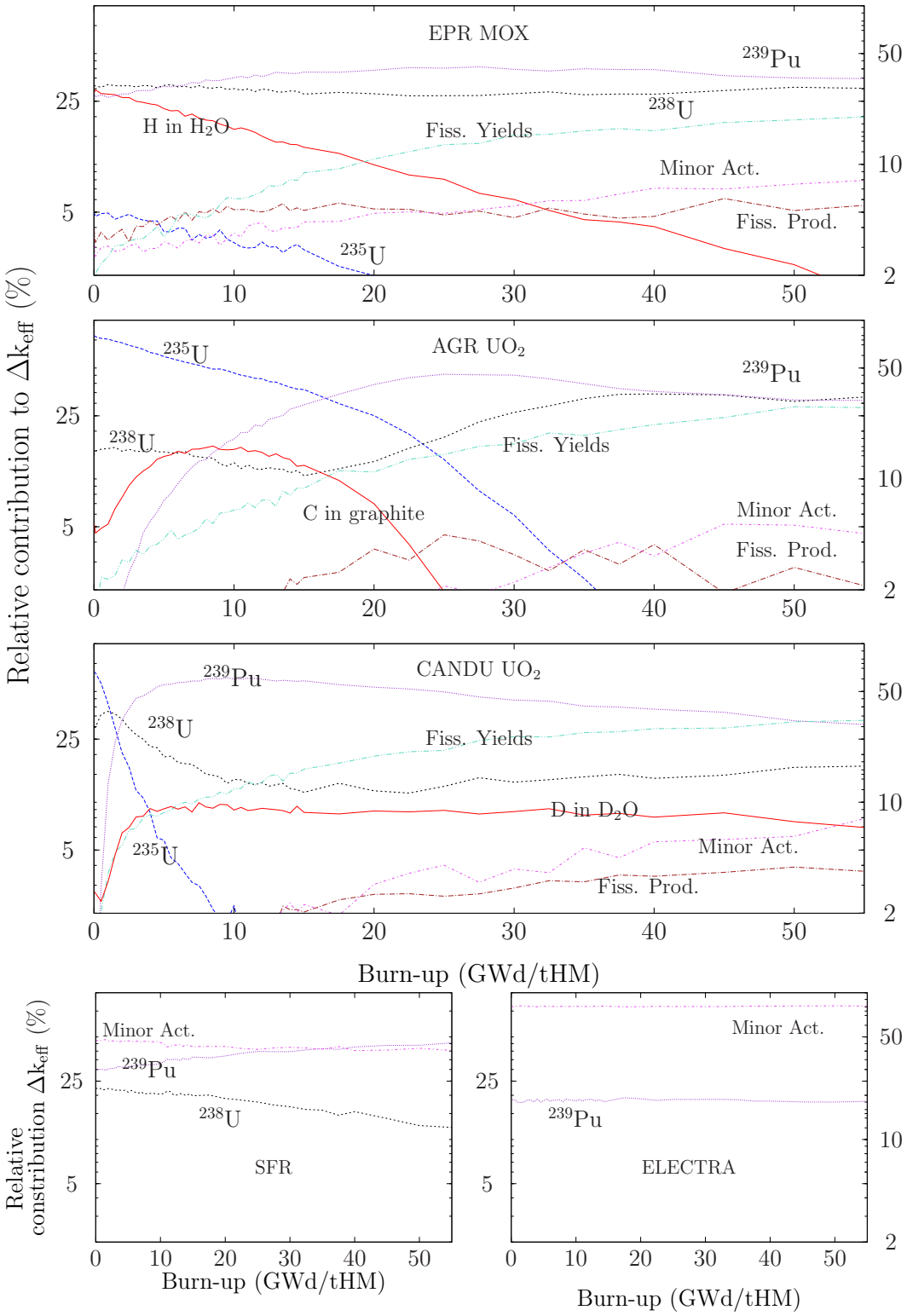

Fig. 5. k_{eff} uncertainties for CANDU, AGR and EPR assemblies, with UO_2 or MOX fuels. The ELECTRA and SFR systems are also presented. Uncertainties are due to $^{235,238}U$, ^{239}Pu, fission products, other actinides and fission yields (no thermal scattering data). The GCFR partial uncertainties are very similar to the ones of the SFR and the ADS partial uncertainties are very similar to the ones of the ELECTRA.

sections) and integral measurements (*e.g.* criticality, burn-up or other benchmarks). These libraries are then used in simulation codes such as SCALE [46], FISPACT, MCNP or SERPENT, showing (very) good agreement with a selection of integral measurements as mentioned in Ref. [42]. The nuclear data uncertainties, as used in this work, are adjusted to differential measurements, but not to integral ones. This naturally leads to uncertainties on integral measurements larger than the bias between calculated integral parameters and the benchmark values.
These results are pointing out that without considering integral information, the uncertainties on reactivity swing due to nuclear data are about 0.55-0.9 % for thermal systems, and could be significantly reduced by including other information, such as experimental uncertainties from integral measurements. Including this type of information in the evaluation of fundamental quantities such as cross sections and their uncertainties is still discussed in the nuclear data evaluation community. It is nevertheless one of the most efficient ways to reduce calculated uncertainties for integral parameters, as presented in Ref. [47].

5 Conclusion

In this study, the uncertainties on the reactivity swing due to nuclear data were calculated with the fast Total Monte Carlo method for 15 different assemblies and cores: 6 thermal assemblies with UO_2 fuel, 5 thermal assemblies with MOX fuel and 4 fast systems. Nuclear data such as actinides, fission products, fission yields and thermal scattering data are considered. Apart from the fast systems of Generation-IV, all uncertainties are within a band of 0.55-0.95 %, either with UO_2 or MOX fuel. The most important impacts come from ^{235,238}U and ^{239}Pu, independently of the considered system, with a non-negligible effect of fission yields and thermal scattering data. For Generation-IV systems, the k_{eff} uncertainties are between 1.4 and 2.4 %, much higher than for thermal systems. The present method can also be applied to calculate uncertainties on any other quantity for which nuclear data have an impact.

References

[1] G.B. Bruna, "Aspects of physics and computation of Plutonium recycling in PWRs: Full MOX loading and Void effect", workshop on nuclear data and nuclear reactors: Physics, design and safety, Trieste, 13 March- 14 April, 2000

[2] J.C. Gehin, J.J. Carbajo and R.J. Ellis, "Issues in the Use of Weapons-Grade MOX Fuel in VVER-1000 Nuclear Reactors: Comparison of UO_2 and MOX Fuels", Oak Ridge National Laboratory, October 2004, ORNL/TM-2004/223.

[3] V. Rouyer, I. Duhamel, G. Poullot, P. Cousinou, F. Barbry, P. Fouillaud and E. Girault, "IRSN projects for critical experiments: Low moderated MOX fuel projects and others", Proceedings of the Int. Conf. on Nuclear Criticality Safety, ICNC 2003, Tokay Mura, Japan, Oct. 20-24, 2003

[4] R.J. Ellis, "VENUS-2 MOX core benchmark: Results of ORNL calculations using HELIOS-1.4, revised report", Oak Ridge National Laboratory, ORNL/TM-2000/180/R1, May 2001.

[5] G.S. Chang, "Weapons-Grade MOX Fuel burnup characteristics in Advanced Test Reactor Irradiation", Idaho National Laboratory, INL/CON-06-01099, July 2006.

[6] K.R. Elam and B.T. Rearden, Nucl. Sci. and Eng. 145, (2003) 196

[7] M. Klein, L. Gallner, B. Krzykacz-Hausmann, A. Pautz and W. Zwermann, "Influence of nuclear data uncertainties on reactor core calculations", Kerntechnik 2011/03, p.174-178

[8] J. Leppänen, 2010, "PSG2 / Serpent - a Continuous-energy Monte Carlo Reactor Physics Burnup Calculation Code", VTT Technical Research Centre of Finland, Finland, http://montecarlo.vtt.fi.

[9] G. Sengler, F. Forêt, G. Schlosser, R. Lisdat and S. Stelletta, "EPR core design", 1999, Nucl. Eng. Design 187, 79

[10] K. Hesketh *et al.*, "Physics of plutonium fuels, BWR MOX benchmark, specification and results, vol. VII," technical report, Nuclear Energy Agency, NSC, 2003.

[11] "Specification for the Phase 1 of a Depletion Calculation Benchmark devoted to Fuel Cycles", NEA/NSC/DOC(2004)11, OECD/NEA (2004).

[12] D. Rochman, A.J. Koning and D.F. da Cruz, Nucl. Techn. 179 (2012) 323.

[13] "Physics of Plutonium, Fueks BWR MOX benchmarks, Specifications and results", Vol. 7, Working Party on Physics of plutonium fuels and innovative fuel cycles, Nuclear Energy Agency, January 2003, ISBN 92-64-19905-5

[14] R. Josek, E. Novak and V. Rypar., "WWER-440 Local Power Peaking Experiment: Benchmark Geometry and Material Specification". UJV Z 1651, NRI, 2006

[15] B. Roque, P. Marimbeau, J.P. Grouiller, "Specification for the Phase 2 of a Depletion Calculation Benchmark devoted to MOX Fuel Cycles." WPRS, NEA/OECD. December 2007.

[16] Pre-Construction Safety Report, chapter 2, http://www.epr-reactor.co.uk

[17] J. Leppänen, "Serpent Progress Report 2010", VTT Technical Research Centre of Finland, Finland, 2010, VTT-R-01362-11.

[18] E. Nonbel, "Description of the Advanced Gas Cooled Reactor (AGR)", Report NKS/RAK2(96)TR-C2, Riso National Laboratory, Roskilde, Denmark, November 1996

[19] J. Wallenius, E. Suvdantsetseg and A. Fokau, Nucl. Techn. 177 (2012) 303

[20] Y. Zhang, "Transmutation of Americium in fast neutron facilities", Licentiate Thesis, Royal Institute of Technology, Stockholm, Sweden, 2011, TRITA-FYS 2011:07.

[21] L.K. Ghasabyan, "Use of Serpent Monte-Carlo code for development of 3D full-core models of Gen-IV fast-spectrum reactors and preparation of group constants for transient analyses with PARCS/TRACE coupled system", Stockholm, Sweden 2013, Master of Science, KTH/FYS/–13:02–SE.

[22] "Fuel Design Evaluation for ATRIUM 1OXM BWR Reload Fuel", ANP-2899NP, AREVA, April 2010

[23] R. Zajac, P. Darilek, V. Necas, Computational Methods in Applied Sciences 24 (2011) 241

[24] A.E. Waltar and A.B. Reynolds, "Fast Breeder Reactors", Pergamon, Press, pp. 776-779, 1981

[25] A. Fokau *et al.*, Ann. of Nucl. Energy, 37 (2010) 540.

[26] A.J. Koning and D. Rochman, Annals of Nucl. Ene. 35 (2008) 2024.

[27] D. Rochman, W. Zwermann, S.C. van der Marck, A.J. Koning, H. Sjöstrand, P. Helgesson and B. Krzykacz-Hausmann, "Efficient use of Monte Carlo: uncertainty propagation", accepted for publication in Nucl. Sci. and Eng., 2014

[28] A.J. Koning and D. Rochman, Nuclear Data Sheets 113 (2012) 2841.

[29] D. Rochman and S.C. Sciolla, "Total Monte Carlo Uncertainty propagation applied to the Phase I-1 burnup calculation", NRG Report 113696, April 2012, Petten, The Netherlands, available at ftp://ftp.nrg.eu/pub/www/talys/bib_rochman/tmc.nrg.pdf.

[30] D. Rochman, A.J. Koning, S.C. van der Marck, Annals of Nucl. Ene. 36 (2009) 810.

[31] D.F. da Cruz, D. Rochman and A.J. Koning., "Uncertainty analysis on reactivity and discharged inventory for a pressurized water reactor fuel assembly due to ^{235,238}U nuclear data uncertainties", in proceedings of the International Congress on the Advances in Nuclear Power Plants June 24-28, 2012, Chicago, Illinois, USA

[32] D. Rochman and A.J. Koning. Nucl. Sci. and Eng. 172 (2012) 287

[33] D. Rochman and A.J. Koning. Nucl. Sci. and Eng., 169 (2011) 68

[34] C.J. Diez, O. Cabellos, D. Rochman, A.J. Koning and J.S. Martinez, Annals of Nucl. Ene. 54 (2013) 27.

[35] D.F. da Cruz, D. Rochman and A.J. Koning, "Uncertainty analysis on reactivity and discharged inventory due to ^{235,238}U, ^{239,240,241}Pu and fission products: application to a pressurized water reactor fuel assembly", accepted for publication in Nucl. Techno., September 2013.

[36] J.B. Briggs, Ed., 2004, International Handbook of evaluated Criticality Safety Benchmark Experiments, NEA/NSC/DOC(95)03/I, Organisation for Economic Co-operation and Development, Nuclear Energy Agency.

[37] "Random nuclear data files", part of the TENDL-2012 distribution, ftp://ftp.nrg.eu/pub/www/talys/tendl2012/random.html, May 2013.

[38] P. Helgesson, D. Rochman, H. Sjöstrand, E. Alhassan, and A.J. Koning, "UO_2 vs. MOX: propagated nuclear data uncertainty for k_{eff}, with burnup", submitted to Nucl. Sci. and Eng., June 2013.

[39] D. Rochman and A.J. Koning., Nucl. Sci. and Eng. **170** (2012) 265.

[40] G. Aliberti *et al.*, Annals of Nucl. Ene. 33 (2006) 700

[41] E. Alhassan, H. Sjöstrand, J. Duan, C. Gustavsson, S. Pomp, M. Österlund, D. Rochman and A.J. Koning, "Uncertainty analysis of Lead cross sections on reactor safety for ELECTRA", Joint International Conference on Supercomputing in Nuclear Applications and Monte Carlo 2013 (SNA+MC 2013), La Cité des Sciences et de l'Industrie, Paris, France, October 27-31, 2013

[42] Second meeting on "Uncertainty propagations in the nuclear fuel cycle", Uppsala University, Sweden, April 24-25, 2013, http://www.physics.uu.se/tk/en/content/meeting-uncertainty-propagations-nuclear-fuel-cycle

[43] M.B. Chadwick, P. Oblozinsky, M. Herman, N.M. Greene, R.D. McKnight, D.L. Smith, P.G. Young, R.E. MacFarlane, G.M. Hale, S.C. Frankle, A.C. Kahler, T. Kawano, R.C. Little, D.G. Madland, P. Moller, R.D. Mosteller, P.R. Page, P. Talou, H. Trellue, M.C. White, W.B. Wilson, R. Arcilla, C.L. Dunford, S.F. Mughabghab, B. Pritychenko, D. Rochman, A.A. Sonzogni, C.R. Lubitz, T.H. Trumbull, J.P. Weinman, D.A. Brown, D.E. Cullen, D.P. Heinrichs, D.P. McNabb, H. Derrien, M.E. Dunn, N.M. Larson, L.C. Leal, A.D. Carlson, R.C. Block, J.B. Briggs, E.T. Cheng, H.C. Huria, M.L. Zerkle, K.S. Kozier, A. Courcelle, V. Pronyaev, S.C. van der Marck, Nuclear Data Sheets **107** (2006) 2931.

[44] K. Shibata, O. Iwamoto, T. Nakagawa, N. Iwamoto, A. Ichihara, S. Kunieda, S. Chiba, K. Furutaka, N. Otuka, T. Ohsawa, T. Murata, H. Matsunobu, A. Zukeran, S. Kamada, and J. Katakura, J. Nucl. Sci. Technol. 48 (2011) 1.

[45] A.J. Koning, D. Rochman, S.C van der Marck, J. Kopecky, J. Ch. Sublet, S. Pomp, H. Sjostrand, R. Forrest, E. Bauge and H. Henriksson, "TENDL-2012: Consistent Talys-based Evaluated Nuclear Data Library including covariances", available at http://www.talys.eu/tendl-2012.

[46] "Scale: A Comprehensive Modeling and Simulation Suite for Nuclear Safety Analysis and Design, Version 6.1", ORNL/TM-2005/39 (2011).

[47] E. Alhassan, H. Sjöstrand, J. Duan, C. Gustavsson, A. Koning, S. Pomp, D. Rochman and M. Österlund, "Combining Total Monte Carlo and Benchmarks for nuclear data uncertainty propagation on an LFRs safety parameters", http://arxiv.org/abs/1303.6563